Available online at www.sciencedirect.com

ScienceDirect

Procedia Manufacturing 15 (2018) 1502–1508

Procedia MANUFACTURING

www.elsevier.com/locate/procedia

17th International Conference on Metal Forming, Metal Forming 2018, 16-19 September 2018, Toyohashi, Japan

Circular simple shear extrusion as an alternative for simple shear extrusion technique for producing bulk nanostructured materials

Ramin Ebrahimi*, Alireza Rezvani, Ebad Bagherpour

Department of Materials Science and Engineering, School of Engineering, Shiraz University, Shiraz, Iran

Abstract

Recently, simple shear extrusion is introduced to fabricate ultrafine-grained materials. It was designed for billets with square cross-sections and was investigated well previously. This study aims to introduce an alternative design of simple shear extrusion process with a circular cross-section, which is named circular simple shear extrusion. The deformation behavior during the new process is investigated by finite element analysis using ABAQUS/Explicit software package. The load of the process and the strain distribution on the processed-sample are studied by a set of simulations. The results show that, in comparison to conventional simple shear extrusion, the circular simple shear extrusion process needs lower extrusion pressures. Also, the accumulated strains are closer to theoretical ones. The amount of friction force in the process with circular cross-section is lower in comparison with the square one which leads to both, the longer service life of the circular simple shear extrusion dies and the lower cost of production. Hence, this new geometry has a strong potential in terms of industrial applications.

Peer-review under responsibility of the scientific committee of the 17th International Conference on Metal Forming.

Keywords: Simple shear extrusion; Severe plastic deformation; Finite element analysis; Circular simple shear extrusion

1. Introduction

An interesting emerging topic in recent years is severe plastic deformation (SPD) which is a powerful tool to fabricate bulk nanostructured or ultra-fine grained materials by imposing large strains to the materials [1,2]. SPD techniques are promising ways to produce materials without any contaminations or porosity. Over the past three

* Corresponding author. Tel.: +98-713-230-3062; fax: +98-713-230-7293.
E-mail address: ebrahimy@shirazu.ac.ir (R. Ebrahimi)

2351-9789
Peer-review under responsibility of the scientific committee of the 17th International Conference on Metal Forming.
10.1016/j.promfg.2018.07.328

decades, several SPD techniques have been studied by many researchers including, equal channel angular pressing (ECAP) [3,4], high pressure torsion [5], accumulative roll bonding [6], cyclic expansion-extrusion [7], twist extrusion (TE) [8] and cyclic extrusion and compression [9].

In 2009, Pardis and Ebrahimi [10] introduced a new SPD technique based on a direct extrusion, named as simple shear extrusion (SSE). It was shown that the amount of waste material in SSEed samples was considerably lower in comparison to ECAPed one. In another study, they introduced four different processing routes A, B, C, and D [11] for SSE. They concluded that the strain homogeneity is better in route C in comparison to route B. In rout C samples are rotated between each passes around extrusion direction by 90°. Bagherpour et al. [12] processed a twinning induced plasticity (TWIP) steel by ECAP and SSE processes. They showed that after one pass of ECAP the segmentation will occur due to flow localization. Since SSE has a quite larger deformation zone, it can deform TWIP steels without producing any segmentation, compared with that of ECAP. This capability is due to the gradual strain imposing in SSE while in ECAP strain imposed abruptly in a narrow region. Bayat Tork et al. [13] investigated the feasibility of plastic deformation of pure magnesium through SSE process at the room temperature. They reported that samples processed by ECAP, channel angular deformation and dual-equal channel lateral extrusion were highly segmented, while the samples processed by SSE showed no significant segmentation. They concluded that SSE is the most promising method for processing and refining the microstructure of magnesium at the room temperature. In another publication, Bagherpour et al. [14] investigated the deformation behavior and microstructural evolution of TWIP steel during SSE technique. They showed that in the first half of the deformation channel, the dislocation density increases and it decreases in the second half due to strain reversal.

Nomenclature

r	radius of the circular cross-section	$\pi/4-\theta$	angle between the major axis of the ellipse and the diagonal of the initial square
L	length of deformation channel	$\pi/4-\theta'$	angle between the major diagonal of the parallelogram and the diagonal of the initial square
γ	shear strain	m	constant friction factor
α	distortion angle	μ	friction coefficient
α_{max}	maximum distortion angle		
β_{max}	maximum inclination angle		

In 2014, various die profiles were proposed by Bagherpour et al. [15] for SSE. By finite element analysis they concluded that the linear die profile is the best choice because of simplicity of the die design, the constant strain rate and homogeneity of the strain. In 2015, Bagherpour et al. [16] introduced a new die parameter named maximum inclination angle, β_{max}. They proposed an analytical model considering the constant friction factor, the maximum distortion angle, the maximum inclination angle and the type of die to predict the optimum die parameters to minimize the load of the process.

In the SPD processes like TE and SSE, the direct extrusion nature of them is a great advantage in industrial lines due to their easy installations. However, both of them have the limitation of their cross sections which should be a square. Although few studies [17-19] tried to apply TE on circular cross-sections, there are not any reports on the application of SSE on the circular cross-sections.

In this paper, a developed design of SSE channel with a circular cross-section, which is named circular simple shear extrusion (CSSE) is proposed. Both SSE and CSSE methods can be utilized on any standard extrusion equipment. It is clear that the circular cross-section is a favorable shape in the most industrial applications. Numerous researchers have investigated strain distributions of the SPD processes using the finite element method [4, 5, 8, 10]. Therefore, a complete comparison between SSE and CSSE has been imposed using finite element code ABAQUS/Explicit.

2. Methodology

2.1. Principles of circular simple shear extrusion

In the SSE process, the specimen undergoes shear strain while it passes through the deformation channel. During the deformation channel, the cross-section area of the sample remains constant. The shear strain reaches its highest value in the middle of the deformation channel where the distortion angle has its highest value of α_{max}. Since the final shape and dimensions of processed samples remain unchanged, it makes it possible to repeat the process as many times to obtain high values of accumulated strain. In the process of the SSE, the shear strain in both halves of the deformation channel is equal and symmetrical. Hence, a shear strain γ_{xy} of $tan(\alpha_{max})$ is applied to the material in each half of the channel. Therefore, according to Mises criterion the total effective strain after one pass of SSE can be calculated by

$$\varepsilon_{eff} = \frac{2\tan(\alpha_{max})}{\sqrt{3}} \quad . \tag{1}$$

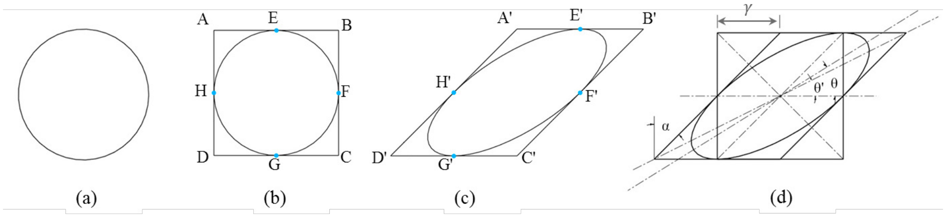

Fig. 1. (a) and (b) initial circular cross-section; (c) and (d) resultant ellipse cross section after imposing the shear strain of γ during CSSE processing

Since the CSSE process is applied to the specimens with an initial circular cross-section, to design the deformation channel for CSSE, the starting point is a circle. Assume an initial circle with the radius of r as shown in Fig. 1(a) as the starting point. There is a square of ABCD (Fig. 1(b)) which is circumscribed about the circle. The circle is contacted to the hypothetical square in 4 points. Applying a shear strain of $tan(\alpha_{max})$ leads the circle to change to an ellipse (E′F′G′H′) of Fig. 1c. This ellipse can be inscribed in A′B′C′D′ parallelogram which is formed by the distortion of the hypothetical square (ABCD) by a distortion angle of α_{max}. The angle between the major axis of the ellipse and the diagonal of the square is $\frac{\pi}{4} - \theta$. Then θ is calculated by [20]

$$\tan(2\theta) = \frac{2}{\gamma} \, . \tag{2}$$

Inserting $\gamma = tan\,\alpha_{max}$ into Eq. (2).

$$\tan(2\theta) = \frac{2}{tan\,\alpha_{max}} \, , \tag{3}$$

where r is the radius of the initial circular cross-section of the die. Also, the angle between the major diagonal of the parallelogram and the diagonal of the initial square is defined as $\frac{\pi}{4} - \theta'$. From the geometry, θ' can be calculated by

$$tan\theta' = \frac{1}{1+\gamma} \, . \tag{4}$$

Inserting $\gamma = tan\,\alpha_{max}$ into Eq. (4), θ' and $tan\,\alpha_{max}$ relate to each other by

$$tan\theta' = \frac{1}{1+tan\,\alpha_{max}} \, . \tag{5}$$

Therefore the angle between the major axis of the ellipse and the major diagonal of the parallelogram is $\theta - \theta'$ which is a non-zero parameter. Combining Eqs. (3) and (5) the relationship between two mentioned angles is determined as

$$tan\theta' = \frac{\tan(2\theta)}{\tan(2\theta)+2} . \tag{6}$$

Another parameter which should be defined for the die fabrication is the length of the deformation channel which is dependent on the maximum inclination and maximum distortion angles as

$$L = \frac{2r\tan\alpha_{max}}{\tan\beta_{max}} \ . \quad (7)$$

In the current study, the CSSE die was designed with r = 5 mm, $\alpha_{max} = 45°$, $\beta_{max} = 22.2°$ and L = 25mm. With this configuration, the initial circular cross-section of the specimen will deform to an elliptical shape at the center of the channel as shown in Fig. 2 and then deform back to its initial circle shape at the outlet. The outlet diameter with small reduction was chosen 9.9 mm to create back-pressure.

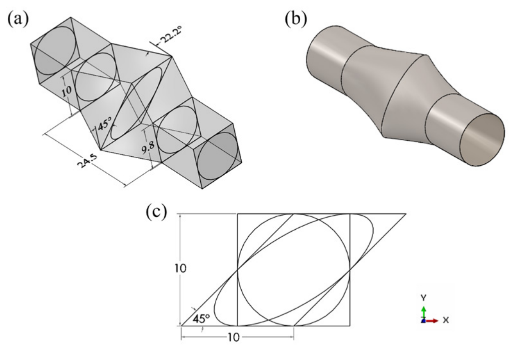

Fig. 2. (a) Geometry of the SSE channel with inscribed shapes (b) geometry of CSSE's deformation channel (c) front view of channel.

Fig. 3. Images of constructed CSSE die and Al-1050 samples before and after deformation by CSSE.

2.2. Finite element analysis

The commercial finite element code ABAQUS/Explicit was used to investigate the deformation behavior during CSSE and SSE processes. Simulations were performed using 3-D models. Die and punch were assumed as rigid bodies and the billets were considered to be a deformable aluminum alloy (AA1050) with the stress-strain relation of $\sigma = 106\ \varepsilon^{0.347}$ MPa [10]. In order to mesh the billet, 8-node linear triangular prism elements (C3D8) [21] were used. The 4-node 3-D bilinear rigid quadrilateral elements (R3D4) were used to mesh the die rigid parts. The back-pressure was considered as 100 MPa. This value was chosen after several simulation in order to find the minimum required back-pressure for filling the die channel. Constant friction factor at the interface between the billet and the die was determined as $m = 0.1$ using barrel compression test [22, 23]. This value was converted to friction coefficient $\mu = 0.047$ by using the following relation to apply in simulation [24].

$$\mu = \frac{m^{0.9}}{2.72(1-m)^{0.11}} \ . \quad (8)$$

2.3. Die design and fabrication

The particular shape of the deformation channel in CSSE technique results in a special design and fabrication method of the corresponding die. Fig. 3 shows the fabricated half dies of the CSSE process and images of Al-1050 samples, before and after deformation by CSSE. As seen, the cutting plane of the deformation channel is a curved one. The reason comes from the problem of "unexposed surface" which is in case of the flat cutting surface. Fig. 4a shows the half ellipse of the middle channel, a half circle of the entrance channel and as an example, an ellipse in the half of deformation channel between these two sections. To cut the channel with a flat surface, the cutting surface should be GEE″G″. By cutting the channel with the flat surface, the area of OE′G′ of the assumed ellipse between the entrance and the middle of the channel (see the circle above Fig. 4(a) could not be machined. Therefore, the surface of Fig. 4b does not exist and this surface is nominally defined as "unexposed surface".

To machine the unexposed surface and have the perfect deformation the cutting surface should be a curved one. To have the aforementioned curved cutting surface, each cross-section of the deformation channel should be cut from the major axis of its corresponding ellipse. In other words, the cutting surface is the surface contains GE, G′E′, G″E″ and all the other major axes of the ellipses.

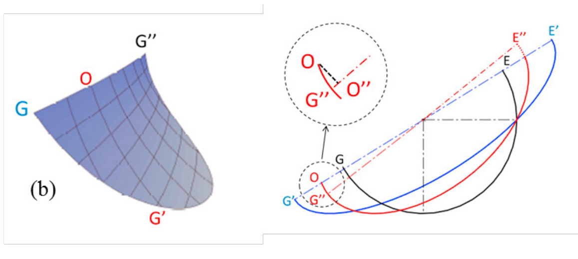

Fig. 4. (a) Illustration of half ellipse of middle channel, half circle of entrance channel and as an example, an ellipse in half of CSSE deformation channel. (b) Representation of unexposed surface formed by cutting deformation channel of CSSE by flat cutting surface.

3. Results and discussion

The distribution of the equivalent strain through the cross-section of the samples after CSSE with and without back-pressure is shown in Fig. 5 As can be seen, the deformation channel was completely filled by imposing 100 MPa of back-pressure. Although heterogeneity is observed radially in the strain distribution of the samples, the distribution of equivalent strain in the sample deformed by CSSE is more uniform and symmetrical in comparison to that of SSE. In both SSE and CSSE the highest amount of strain is achieved in the center [10]. The authors would like to draw the attention of the readers to this fact that the nature of almost all of SPD techniques imposes a non-uniform strain to the material. However, the strain distribution in SSEed and CSSEed samples is more uniform in comparison to the samples processed by the other SPD methods such as, TE, HPT and ECAP.

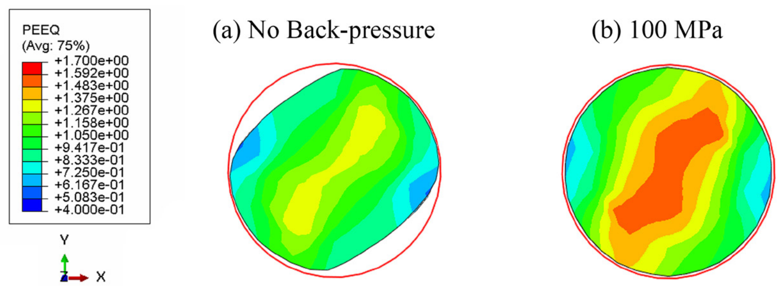

Fig. 5. Accumulative strain distribution in a cross-section of CSSE processed samples (a) without back-pressure (b) with back-pressure of 100 MPa.

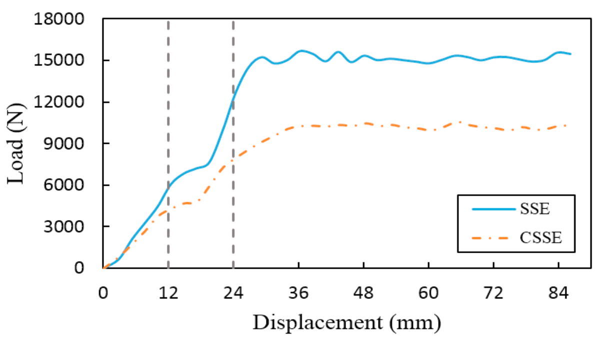

Fig. 6. Comparison of processing load between SSE and CSSE.

Fig. 6 shows the processing load against ram displacement of both SSE and CSSE processes. As seen in this figure, the required force for the CSSE process is lower than that of SSE. It should be noted that friction is a factor that increases the processing load. Since frictional force is a function of surface area, decreasing the surface area will decrease the amount of this force. Due to the fact that cylindrical specimens have less surface area in comparison with prismatic ones, the friction force in CSSE process is less than SSE. Hence the total force of CSSE becomes lower than the total force of the SSE process. Another cause of this reduction in force is the smaller cross-sectional area of cylindrical samples. According to the length of the deformation channel, this curve can be divided into three regions, the first region represents the load required for the specimen as it fills the first half of the deformation channel. In the second region as the specimen continues to fill the second half of the channel the load increases. In the third region since the deformation channel has completely filled with specimens, the load reaches the steady state condition.

4. Conclusions

Circular simple shear extrusion (CSSE) is introduced as an alternative of simple shear extrusion (SSE). While SSE process is capable to deform the specimens with square cross sections, CSSE is presented to deform workpieces with the circular cross-section. Since the circular cross-section is a favorable shape in the most industrial applications, CSSE process is of great importance in industrial applications. The concepts of the process and die design is explained in detail in order to easy reconstruction of the die. Another advantage of CSSE process is its processing load which is substantially lower than that of SSE. The distribution of strain in CSSE processed sample has the same trend as the SSE processed one.

Acknowledgments

The authors appreciate Shiraz University for financial support (grant number 96-GR-ENG-15) and research facilities used in this work.

References

[1] Y. Zhu, R.Z. Valiev, T.G. Langdon, N. Tsuji, K. Lu, Processing of nanostructured metals and alloys via plastic deformation, MRS BULLETIN, 35 (2010) 977–981.
[2] R.Z. Valiev, The new trends in fabrication of bulk nanostructured materials by SPD processing, Journal of Materials Science, 42 (2007) 1483–1490.
[3] V.M. Segal, Materials processing by simple shear, Materials Science and Engineering:A, 197 (1995) 157–164.
[4] F. Kang, J.T. Wang, Y.L. Su, K.N. Xia, Finite element analysis of the effect of back pressure during equal channel angular pressing, Journal of Materials Science, 42 (2007) 1491–1500.
[5] D. . Lee, H.S. Kim, Finite element analysis for the geometry effect on strain inhomogeneity during high-pressure torsion, Journal of Materials Science, 49 (2014) 6620–6628.
[6] Y. Saito, N. Tsuji, H. Utsunomiya, T. Sakai, R. G. Hong, Ultra-fine grained bulk aluminum produced by accumulative roll-bonding (ARB) process, Scripta Materialia, 39 (1998) 1221–1227.
[7] N. Pardis, B. Talebanpour, R. Ebrahimi, S. Zomorodian, Cyclic expansion-extrusion (CEE): A modified counterpart of cyclic extrusion-compression (CEC), Materials Science and Engineering: A, 528 (2011) 7537–7540.
[8] M.I. Latypov, I.V. Alexandrov, Y.E. Beygelzimer, S. Lee, H.S. Kim, Finite element analysis of plastic deformation in twist extrusion, Computational Materials Science, 60 (2012) 194–200.
[9] Y. Chen, Q. Wang, J. Lin, L. Zhang, C. Zhai, Fabrication of bulk UFG magnesium alloys by cyclic extrusion compression, Journal of Materials Science, 42 (2007) 7601–7603.
[10] N. Pardis, R. Ebrahimi, Deformation behavior in Simple Shear Extrusion (SSE) as a new severe plastic deformation technique, Materials Science and Engineering: A, 527 (2009) 355–360.
[11] N. Pardis, R. Ebrahimi, Different processing routes for deformation via simple shear extrusion (SSE), Materials Science and Engineering: A, 527 (2010) 6153–6156.
[12] E. Bagherpour, M. Reihanian, R. Ebrahimi, On the capability of severe plastic deformation of twining induced plasticity (TWIP) steel, Materials & Design 36 (2012) 391–395.
[13] N.B. Tork, N. Pardis, R. Ebrahimi, Investigation on the feasibility of room temperature plastic deformation of pure magnesium by simple shear extrusion process, Materials Science and Engineering: A, 560 (2013) 34–39.
[14] E. Bagherpour, M. Reihanian, R. Ebrahimi, Processing twining induced plasticity steel through simple shear extrusion, Materials & Design, 40 (2012) 262–267.
[15] E. Bagherpour, F. Qods, R. Ebrahimi, Effect of geometric parameters on deformation behavior of simple shear extrusion, IOP Conference Series: Materials Science and Engineering, 63 (2014) 012046.

[16] E. Bagherpour, R. Ebrahimi, F. Qods, An analytical approach for simple shear extrusion process with a linear die profile, Materials & Design, 83 (2015) 368–376.
[17] C. Wang, F. Li, Q. Li, J. Li, L. Wang, J. Dong, A novel severe plastic deformation method for fabricating ultrafine grained pure copper, Materials & Design, 43 (2013) 492–498.
[18] W. Chengpeng, L. Fuguo, L. Hongya, Y. Zhanwei, C. Bo, Q. Huijuan, Deformation analysis of elliptical cross-section spiral equal-channel extrusion technique, Rare Metal Materials and Engineering, 42 (2013) 0679–0683.
[19] M.I. Latypov, Y. Beygelzimer, H.S. Kim, Comparative analysis of two twist-based SPD processes: Elliptical Cross-Section Spiral Equal-Channel Extrusion vs. Twist Extrusion, Materials Transactions, 54 (2013) 1587–1591.
[20] J.J. Jonas, C. Ghosh, S. Shrivastava, Problems with Using the Hencky Equivalent Strain in Simple Shear, Materials Transactions, 52 (2011) 1748–1751.
[21] ABAQUS™/CAE User's Manual. Dassault Systems. ABAQUS™ Ver. 6.14
[22] R. Ebrahimi, A. Najafizadeh, A new method for evaluation of friction in bulk metal forming, Journal of Materials Processing Technology, 152 (2004) 136–143.
[23] S. Molaei, R. Ebrahimi, Z. Abbasi, Upper bound analysis of barrel compression test using a new velocity field, Iranian Journal of Science and Technology, Transactions of Mechanical Engineering, 40 (2016) 1–10.
[24] S. H. Molaei, M. Shahbaz, R. Ebrahimi, The relationship between constant friction factor and coefficient of friction in metal forming using finite element analysis, Iranian Journal of Materials Forming, 1 (2014) 14–22.